Toward a first-principles understanding of cold nuclear matter effects

Ivan Vitev, LANL

W. Ke, I.V., ArXiV:2301.11940, W. Ke, J. Terry, I.V., ArXiV:2408.10310,

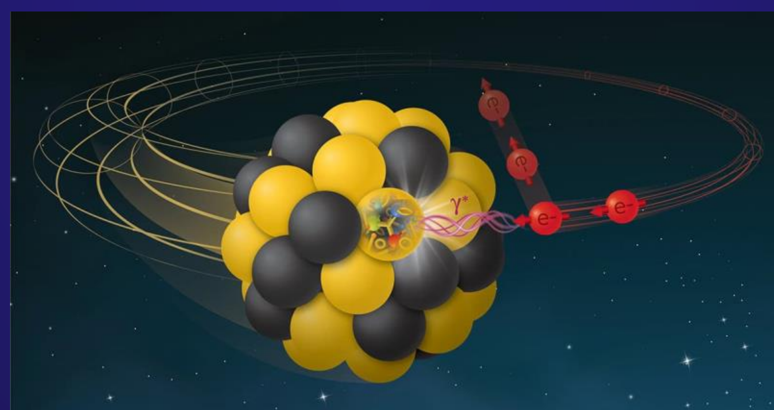

CFNS workshop: Cold Nuclear Matter Effects: from the LHC to the EIC
Stony Brook, NY Jan. 13 – 16, 2025

Collinear and TMD DIS and DY in eA and pA, and CNM effects

Our goal is to calculate collinear and TMD DIS and DY in eA and pA reactions. Understand cold nuclear matter effects that can be calculated perturbatively (at least partly)

- Some can be of leading twist nature parametrized in nPDFs

  See talks in yesterday's session, refs therein

- Many can be understood form the coherent, incoherent and inelastic scattering in nuclei

  See talks in today's and some in yesterday's sessions, refs therein

I. Vitev et al. (2002)

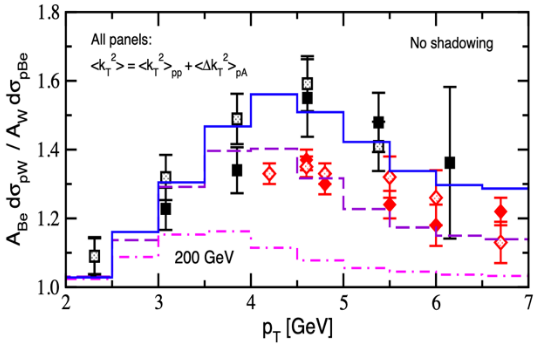

Cronin effect

Goal is to combine in a unified first principles formalism

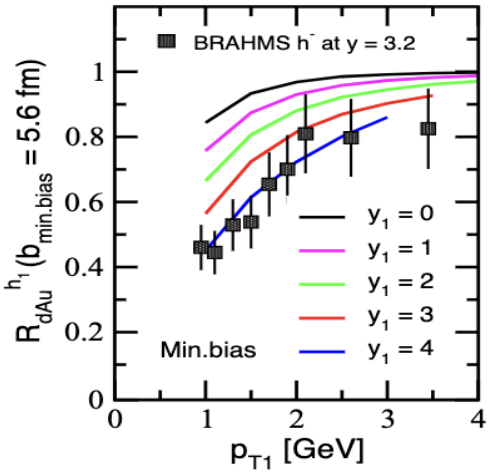

Coherent power corrections

J. Qiu et al. (2005)

B. Neufeld et al. (2010)

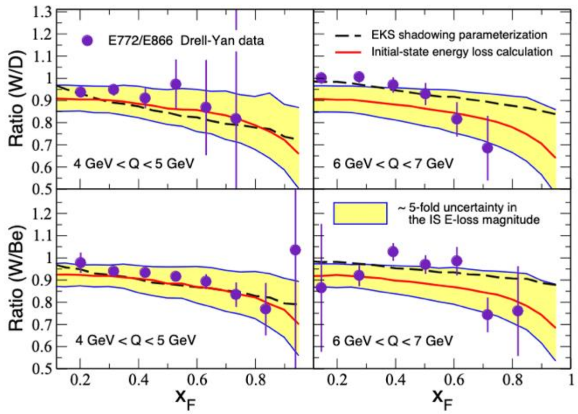

Energy loss

The renormalization group

Much of the reported work is based on renormalization group (RG) analysis

The theory of how to connect physics at different scales. Applicable to “a number of problems in science which have, as a common characteristic, that complex microscopic behavior underlies macroscopic effects.”

K. Willson (1982)
Nobel Prize speech

Origins can be traced to:

Ideas of scale transformations in QED

M. Gell-Man, I. Low (1954)

Handling infinities in field theories

R. Feynman, J. Schwinger, S. Tomonaga, Nobel Prize (1965)

- Hydrodynamics — *V. Yakhot et al. (1986)*
- Social networks — *M. Newman et al. (1999)*
- Low energy nuclear physics — *S. Bogner et al. (2007)*
- Small-x physics — *J. Jalilian-Marian et al. (1998)*

In particle and nuclear physics – a way of making sense of inherently divergent theories

Scales in the in-medium parton shower problem

Calculations have been done using energy loss, in-medium DGLAP, etc. Our goal is to gain an analytic understanding of the problem

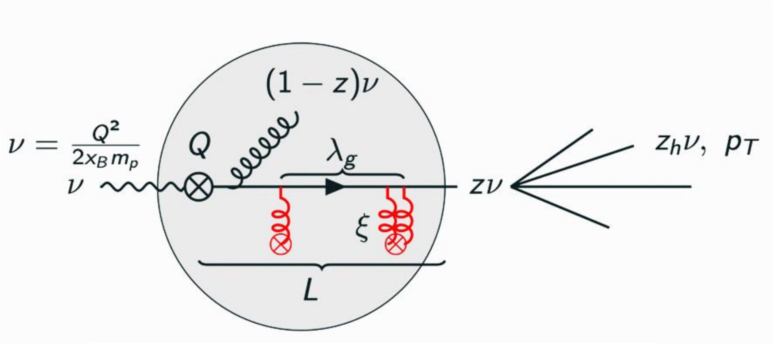

Useful picture of DIS on A

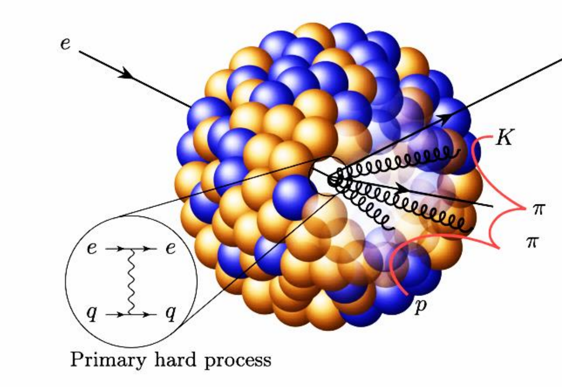

Pretty picture of DIS on A

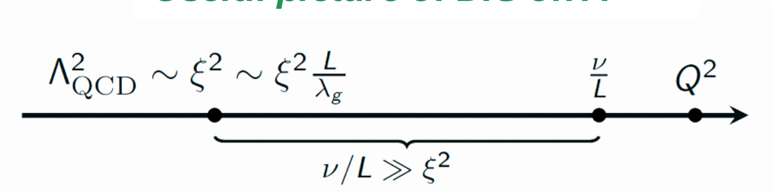

- Medium-size sensitive modes have $p^- \sim \frac{1}{L} \Longrightarrow \lambda = \frac{1}{\sqrt{\nu L}}$.
  - $p_c^2 \sim q^2 \sim \nu \cdot \frac{1}{L}$ a semi-hard scale for thin medium!
  - $p_s^2 \sim 1/L^2$, non-perturbative.

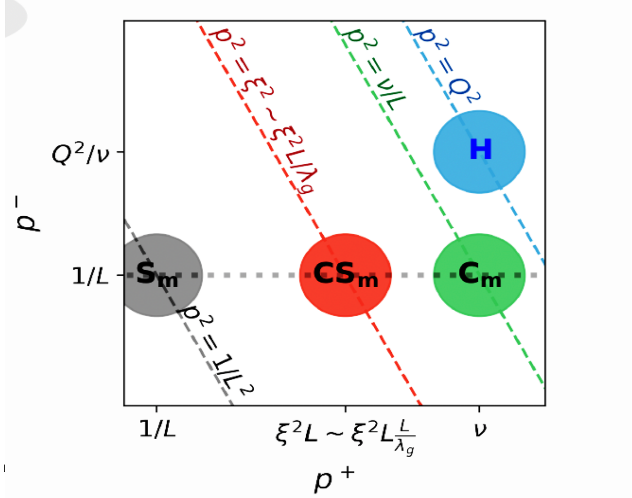

Modes in the virtuality plane

We encounter many ratios of scales in DIS on nuclei. Will resum large logarithms of Q/Qo and E/ξ^2L

Diagrams for the collinear matching coefficient function

We need to evaluate diagrams that impart transverse momentum via collisions (Glauber gluons) or radiation (or not). SCET$_G$ sufficient

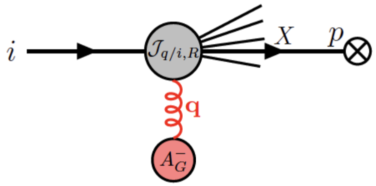

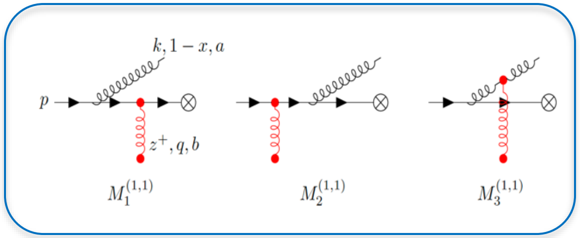

Single Glauber, real radiation

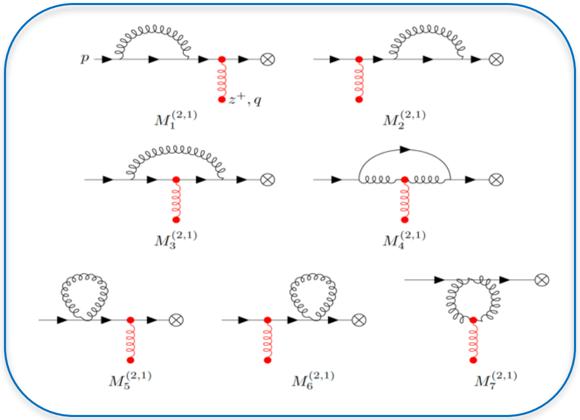

Single Glauber, loop correction

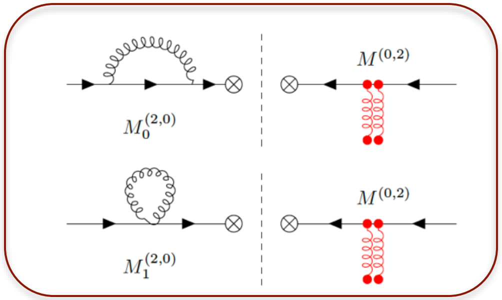

Wavefunction renormalization

Vanishes to leading power (scales integrals)

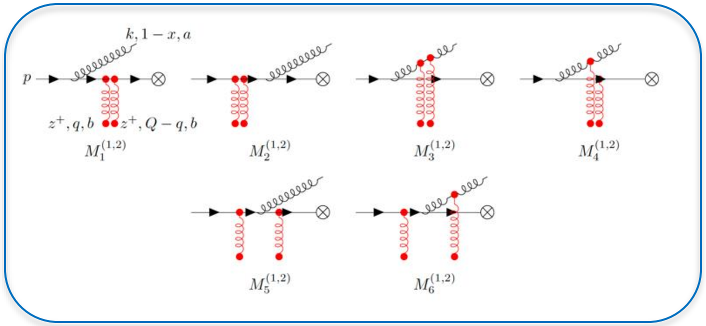

Double Glauber, real radiation

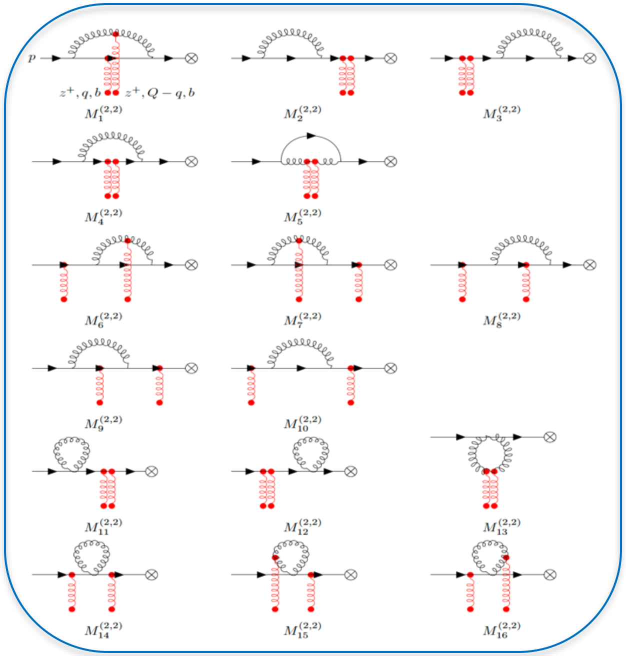

Double Glauber, loop correction

- New direct calculation of loop diagrams

Disclaimers: a) the diagrams are drawn for DY, but they are essentially the same for DIS; b) for the collinear calculation we integrate over the transverse momenta

Technical aspect one: the splitting functions

The diagrams add to contributions proportional to the in-medium splitting functions

In cold nuclear matter (uniform density) we can analytically integrate over the path length. We can can significantly simplify the propagator and phase structure that arises form in-medium interactions

Up to color and kinematic factors, the splitting functions have the same universal form

$i \to j$	$C_1^{ij},\ (\Delta_1^{ij})^2$	$C_2^{ij},\ (\Delta_2^{ij})^2$	$C_3^{ij},\ (\Delta_3^{ij})^2$
$q \to q$	$C_A,\ x^2$	$C_A,\ 1$	$2C_F - C_A,\ (1-x)^2$
$q \to g$	$C_A,\ 1$	$C_A,\ (1-x)^2$	$2C_F - C_A,\ x^2$
$g \to q$	$C_A,\ (1-x)^2$	$C_A,\ x^2$	$2C_F - C_A,\ 1$
$g \to g$	$C_A,\ 1$	$C_A,\ x^2$	$C_A,\ (1-x)^2$

$$P_{ij}^{(1)}(x,E,\mu_2^2) = \frac{\alpha_s^{(0)} P_{ij}(x)}{2\pi^2} L \int \frac{\mu_2^{2\epsilon} d^{2-2\epsilon}\mathbf{k}}{(2\pi)^{-2\epsilon}} \frac{\Phi\left[\frac{\mathbf{k}^2 L}{2x(1-x)E}\right]}{\mathbf{k}^2}$$
$$\times \sum_n \int \frac{\mu_2^{2\epsilon} d^{2-2\epsilon}\mathbf{q}}{(2\pi)^{-2\epsilon}} \frac{\rho_G \alpha_s^{(0)} C_n^{ij} \Delta_n^{ij}(x)}{\pi(\mathbf{q}^2+\xi^2)^2} \frac{\mathbf{q}\cdot[\mathbf{k}+\Delta_n^{ij}(x)\mathbf{q}]}{[\mathbf{k}+\Delta_n^{ij}(x)\mathbf{q}]^2}$$

The remaining integration over the momentum exchanges with the can be performed using dim. reg. and by expanding the integrand

Final result

$$P_{ij}^{(1)}(x,E,\mu_2^2) = \frac{\alpha_s^2(\mu_2^2)\rho_G L}{8E/L} \frac{P_{ij}(x)}{[x(1-x)]^{1+2\epsilon}} \left[\frac{\mu_2^2 L}{\chi(w)E}\right]^{2\epsilon}$$
$$\times B(w) \sum_n C_n^{ij} [\Delta_n^{ij}(x)]^{2-2\epsilon} (1+\mathcal{O}(\epsilon^2))(1+\mathcal{O}(v))$$

Slowly varying functions O(one/few)

$$\int_0^w du \frac{4}{\pi} \frac{\Phi(u)}{u^{2+2\epsilon}} = B(w)[\chi(w)/2]^{-2\epsilon} + \mathcal{O}(\epsilon^2)$$

$$B(w) = \frac{4}{\pi}\int_0^w \Phi(x)\frac{dx}{x^2}, \quad \chi(w) = 2\exp\left\{\frac{1}{B(w)}\frac{4}{\pi}\int_0^w \Phi(x)\ln(x)\frac{dx}{x^2}\right\}$$

One important part here is the additional 1/x(1-x) divergence at the endpoints of the splitting function

Technical aspect two: the subtraction of divergences

Take the flavor non-singlet distribution for simplicity

$$\Delta F_{\rm NS}^{\rm med}(z) = \int_z^1 \frac{dx}{x} F_{\rm NS}(\frac{z}{x}) P_{qq}^{\rm med(1)}(x) \quad + \quad \text{virtual term.}$$

$$P_{qq}^{\rm med(1)}(x) = A(\alpha_s, \cdots) \cdot \frac{P_{qq}^{vac(0)}(x)}{[x(1-x)]^{1+2\epsilon}} \cdot \left[\frac{\mu^2 L}{\chi z \nu}\right]^{2\epsilon} \cdot C_n \Delta_n(x)$$

Define a generalized + prescription and a subtracted function so that the integral with endpoint divergences is finite

$$\int_0^1 \frac{G(x)}{x^{1+2\epsilon}(1-x)^{2+2\epsilon}} dx = \int_0^1 \frac{\{G(x)\}_{qq}}{x(1-x)^2} dx - \frac{G(0)}{2\epsilon} + \frac{G'(1)}{2\epsilon} - G(1)\left(\frac{1}{2\epsilon} + 2\right) + \mathcal{O}(\epsilon).$$

$$\{G(x)\}_{qq} = G(x) - (1-x)^2 G(0) - x(2-x)G(1) - x(x-1)G'(1).$$

The large medium induced logarithms that need to be resummed

The 1/ε divergence and M^(1) counter term that is determined to cancel it. It arises from the soft-collinear sector $(p_{\rm cs}^2 \sim \xi^2 ... \xi^2 L/\lambda_g)$

$$\Delta F_{\rm NS} = \frac{\alpha_s^2 B(w) \rho_G L}{8\nu/L}\left(\frac{1}{2\epsilon} + \ln\frac{\mu_2^2 L}{\chi z \nu}\right) 2C_F \left(\frac{2C_A + C_F}{z} - 2C_A \frac{d}{dz}\right) F_{\rm NS}(z) + \int_0^1 \frac{dy}{y} F_{\rm NS}(y) M_{qq}^{(1)}\left(\frac{z}{y}, \mu_2, z\nu\right)$$
$$+ \frac{\alpha_s^2 B(w) \rho_G L}{8\nu/L} C_F \left[\int_0^1 \frac{\left\{\sum_n C_n^{qq} [\Delta_n^{qq}(x)]^2 (1+x^2) \left[\frac{x}{z} F_{\rm NS}\left(\frac{z}{x}\right) - \frac{F_{\rm NS}(z)}{z}\right]\right\}_{qq}}{x(1-x)^2} dx + \frac{(4C_A - C_F) F_{\rm NS}(z)}{z}\right].$$

Fixed order contribution - free of divergences, no large log enhancement

In-medium collinear RG evolution

- **Derived a full new set of RG evolution equations. The NS distribution has a very elegant traveling wave solution**

$$F_{\rm NS}(\tau, z) = \frac{F_{\rm NS}\left(0, z + 4C_F C_A \tau\right)}{\left(1 + 4C_F C_A \tau / z\right)^{1 + C_F/(2C_A)}}$$

Suitable change of variables. Also captures the density, path length and energy dependence

$$\tau(\mu^2) = \frac{B(w)\rho_G^- L^+}{8p_1^+/L^+}\frac{4\pi}{\beta_0}\left[\alpha_s(\mu^2) - \alpha_s\left(\frac{\gamma(w)p_1^+}{L^+}\right)\right]$$

Flavor non-singlet (q-qbar) **Flavor singlet (q+qbar, g)**

$$\frac{\partial F_{q-\bar{q}}}{\partial \tau} = \left(4C_F C_A \frac{\partial}{\partial x} - \frac{4C_F C_A}{x} - \frac{2C_F^2}{x}\right) F_{q-\bar{q}}$$

$$\frac{\partial F_{q+\bar{q}}}{\partial \tau} = \left(4C_F C_A \frac{\partial}{\partial x} - \frac{4C_F C_A}{x} - \frac{2C_F^2}{x}\right) F_{q+\bar{q}} + \frac{2C_F T_F}{x} F_g,$$

$$\frac{\partial F_g}{\partial \tau} = \left(4C_A^2 \frac{\partial}{\partial x} - \frac{2N_f C_F}{x}\right) F_g + \sum_q \frac{2C_F^2}{x} F_{q+\bar{q}}.$$

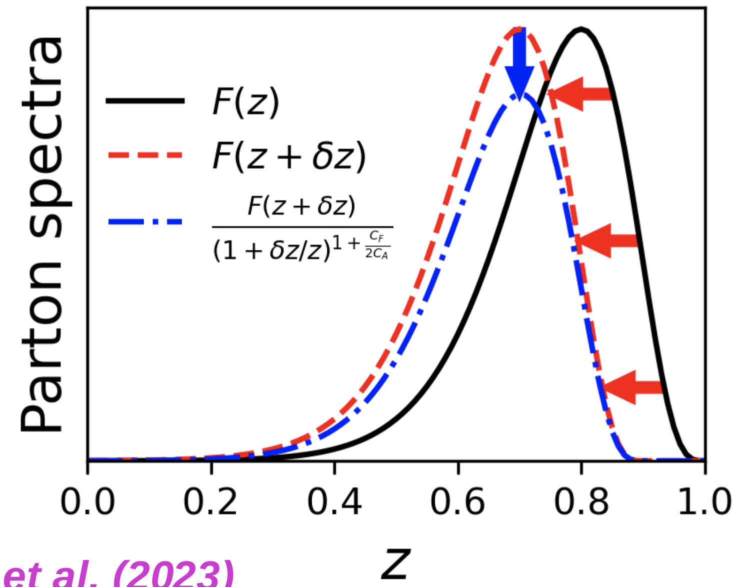

W. Ke et al. (2023)

Can directly identify parton energy loss, the nuclear size dependence of the modification, etc

- Connection between RHIC/LHC (hadronic collisions) and EIC (DIS): The same in-medium RG evolution describes the suppression of hadron production in SIDIS on nuclei and DY in pA

Phenomenological applications of the new RG analysis to HERMES

Revisiting the HERMES data

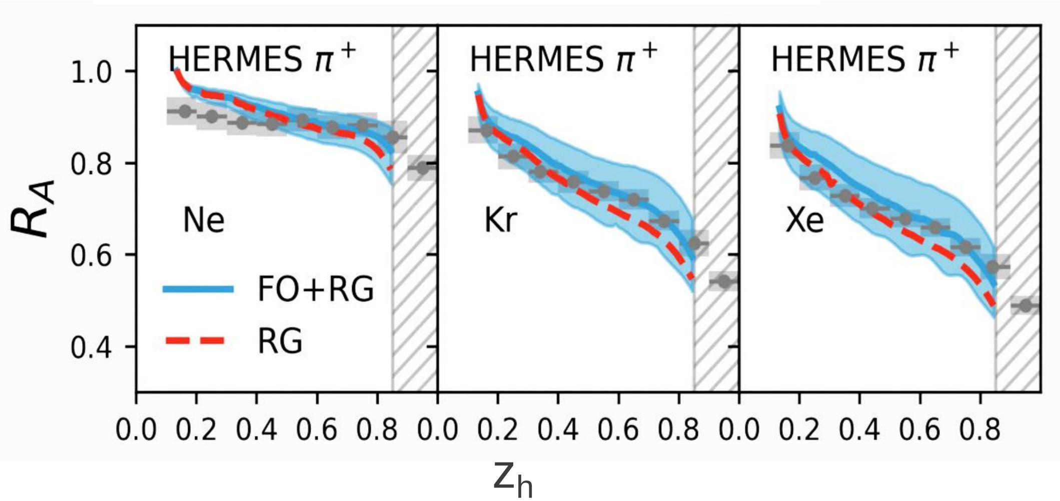

Observable chosen to eliminate initial-state effects

$$R^{\pi}_{eA}(\nu, Q^2, z) = \frac{\left.\frac{N^{\pi}(\nu,Q^2,z)}{N^{e}(\nu,Q^2)}\right|_A}{\left.\frac{N^{\pi}(\nu,Q^2,z)}{N^{e}(\nu,Q^2)}\right|_D}$$

- RG evolution gives a good description of the data at small to intermediate z_h .
- Fixed order corrections improve the agreement at large z_h

W. Ke et al. (2023)

RG evolution advantages

- The method is systematically improvable – both higher logarithmic accuracy and fixed order terms, if higher order splitting functions are available
- Numerically, it is much faster to implement and solve in comparison to in-medium DGLAP evolution
- The proper in-medium scale separation increases predictive power
- At the level of cross sections one can identify the effects of “energy loss”

Practical concerns (not specific to the RG approach)

- The scales of the medium (lower boundary) are small and the coupling strong

Demonstration of predictive power

Addressing EMC data

- EMC measurement for C, Cu, and Sn nuclei at similar x_B much higher $Q^2 \sim 11$ GeV^2
- Same effective Glauber gluon density used

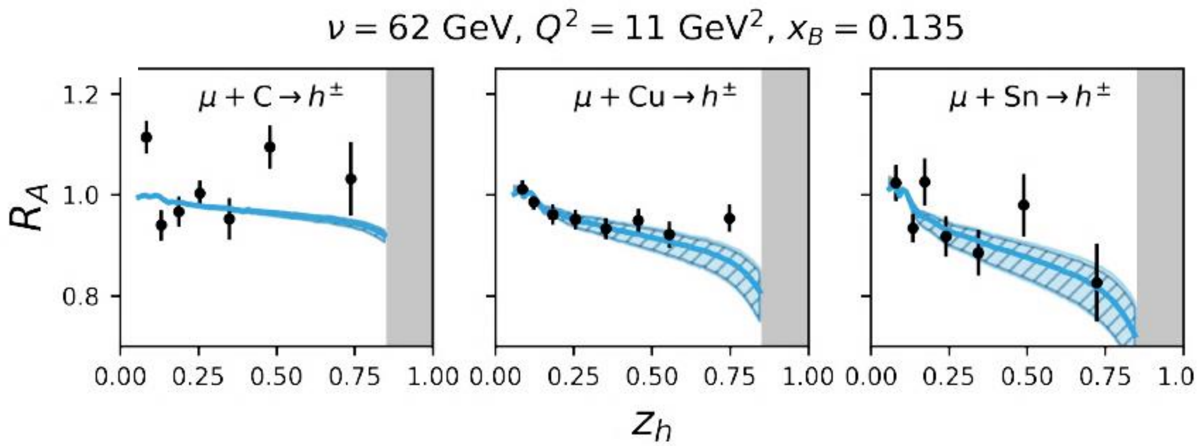

Fixed order (FO) + RG evolution compared to EMC data

Predictions for the EIC

- The modifications to hadronization at EIC depends on kinematics x_B,Q^2
- At large x_B and (forward rapidities) the modification can be very significant

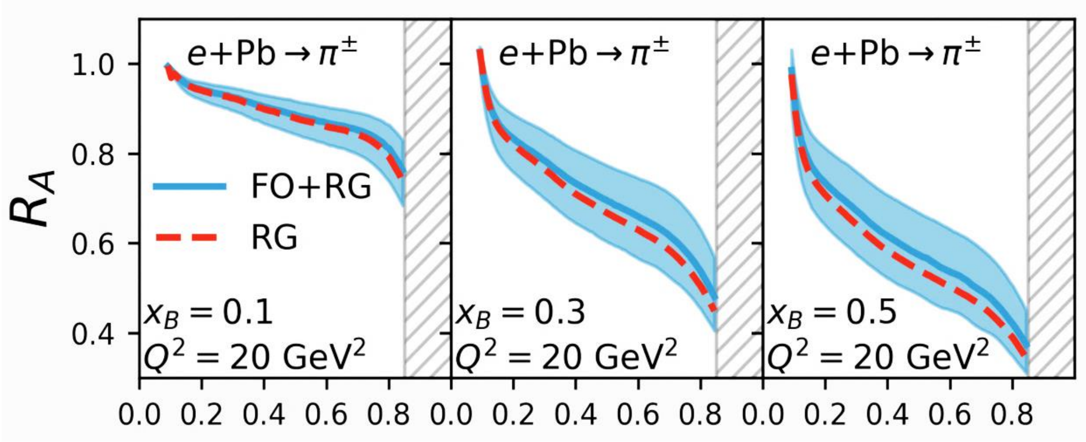

W. Ke et al. (2023)

Factorization in SCET for the TMD DY

Factorized expression, impact parameter space

$$\frac{d\sigma}{dy\, dQ^2\, d^2\mathbf{P}_T} = \sigma_0(Q, \sqrt{s}) H(Q,\mu) \sum_q c_q(Q) \int \frac{d^2\mathbf{b}}{(2\pi)^2} e^{i\mathbf{b}\cdot\mathbf{P}_T}$$
$$\times \mathcal{B}_{q/a}\left(x_1, b, \mu, \frac{\zeta_1}{\nu^2}\right) \mathcal{B}_{\bar{q}/b}\left(x_2, b, \mu, \frac{\zeta_2}{\nu^2}\right) S(b,\mu,\nu)$$

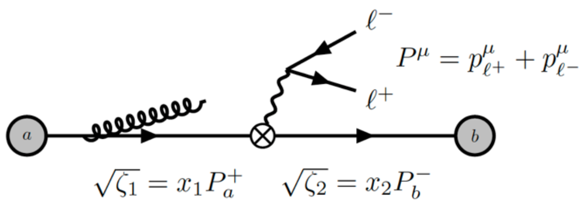

R. Boussarie et al. (2023)

- Total cross section coefficient (Born level cross section) $\sigma_0(Q, \sqrt{s}) = \dfrac{4\pi\alpha_{\rm em}^2}{3N_c Q^2 s}$
- Hard part and charge coefficient (only non-trivial when one reaches electroweak scales)
- Beam function that matches on the collinear PDF in the perturbative region

$$\mathcal{B}_{q/a}\left(x, b, \mu, \frac{\zeta_1}{\nu^2}\right) = \frac{1}{2N_c} \int \frac{d^4z}{2\pi} e^{iz\cdot p} \delta(n\cdot z)\, \delta^2(\mathbf{z}_T - \mathbf{b})\, \mathrm{Tr}\left[\left\langle P_a \left| \bar{\chi}_n(z) \frac{\not{\bar{n}}}{2} \chi_n(0) \right| P_a \right\rangle\right]$$

$$\mathcal{B}_{q/a}\left(x_1, b, \mu, \frac{\zeta_1}{\nu^2}\right) = \sum_i \int_{x_1}^1 \frac{dx}{x} C_{q/i}\left(x, b, \mu, \mu_i, \frac{\zeta_1}{\nu^2}\right) f_{i/a}\left(\frac{x_1}{x}, \mu_i\right) + \mathcal{O}(b^2\Lambda^2_{\rm QCD})$$

- Soft function (with a staple Willson line because $S(\mathbf{b},\mu,\nu) = \dfrac{1}{N_c}\langle 0|\, \mathrm{Tr}\left[W_{\gg}(\mathbf{b})\right] |0\rangle$

Evolution and pp example

Modes and scales in TMD DY

$$p_c \sim Q\left(1, \lambda^2, \lambda\right), \qquad p_{\bar{c}} \sim Q\left(\lambda^2, 1, \lambda\right), \qquad p_s \sim Q\left(\lambda, \lambda, \lambda\right)$$

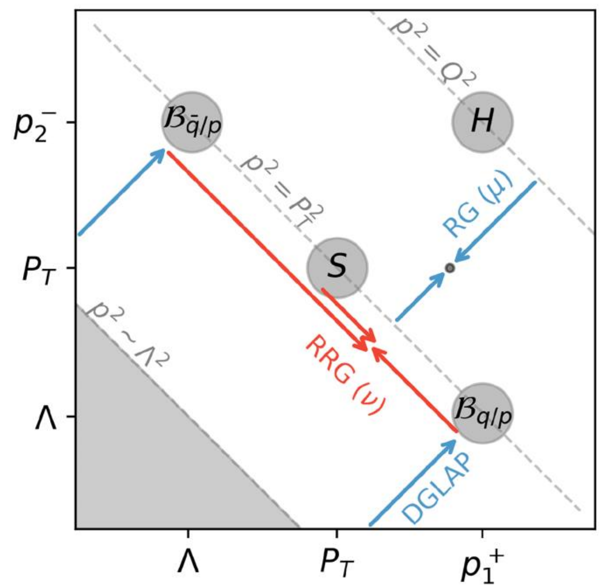

RG

$$\frac{d}{d\ln\mu}\ln H(Q,\mu) = \gamma_\mu^H(Q,\mu),$$

$$\frac{d}{d\ln\mu}\ln \mathcal{B}\left(x, b, \mu, \frac{\zeta}{\nu^2}\right) = \gamma_\mu^B\left(\mu, \frac{\zeta}{\nu^2}\right),$$

$$\frac{d}{d\ln\mu}\ln S\left(b, \mu, \nu\right) = \gamma_\mu^S\left(\mu, \frac{\mu}{\nu}\right).$$

RRG

$$\frac{d\ln\mathcal{B}}{d\ln\nu} = \gamma_\nu^B(b,\mu),$$

$$\frac{d\ln S}{d\ln\nu} = \gamma_\nu^S(b,\mu)$$

J. Chiu et al. (2012)

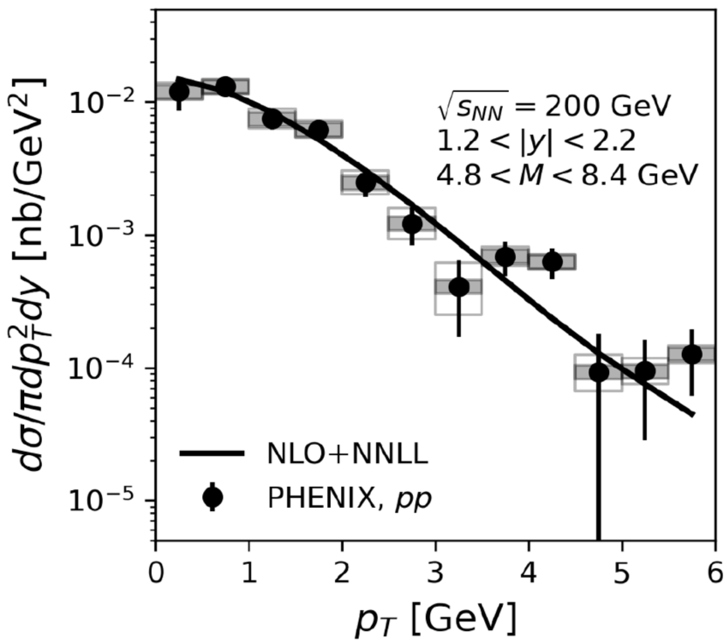

Comparison to the PHENIX data

- Note the emergence of the Collins-Soper scales (CS)

$$\sqrt{\zeta_1} = p_a^+ \text{ and } \sqrt{\zeta_2} = p_b^- \text{ with } \sqrt{\zeta_1\zeta_2} = Q^2$$

- Evolution is controlled by renormalization group (RG) and rapidity renormalization group (RRG) equations

NLO+NNLL code with NP effects *M. Alrashed et al. (2021)*

$$S_{\rm NP}^f(\mathbf{b}, Q) = \frac{g_2}{2}\ln\frac{b}{b^*}\ln\frac{\sqrt{\zeta}}{\sqrt{\zeta_0}} + g_1^f \mathbf{b}^2 \qquad b^* = \frac{b}{\sqrt{1 + b^2/b_{\rm max}^2}}, \qquad \mu_b^* = 2e^{-\gamma_E}/b^*.$$

Note that as we go to high p_T we will underpredict the data. Not matched to collinear calculation (the "Y" term)

Structure of the calculation in matter

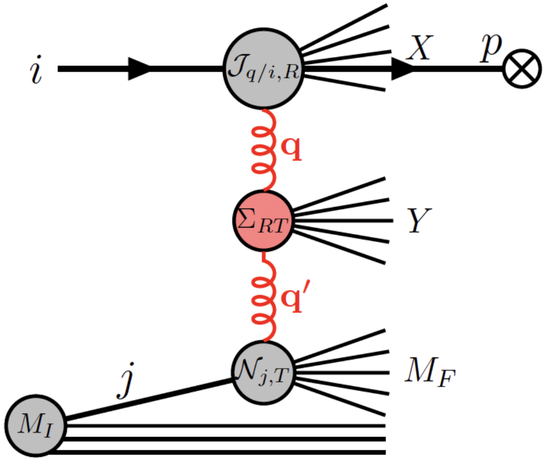

Take the opacity expansion approach and calculate the correction to the proton beam function

Factorized expression for first order in opacity correction

$$\mathcal{B}_{q/a} = \mathcal{B}_{q/a,0} + \chi\, \mathcal{B}_{q/a,1} + \cdots$$

$$\frac{d\sigma_1}{d\mathcal{PS}} = \frac{4\pi\alpha_{\rm em}^2}{3N_c Q^2 s} H(Q,\mu) \sum_q c_q(Q) \int \frac{d^2\mathbf{b}}{(2\pi)^2} e^{i\mathbf{P}_T\cdot\mathbf{b}} \times \sum_{N\in A} \mathcal{B}_{q/p,1}\left(x_1, b, \mu, \frac{\zeta_1}{\nu^2}; \mu_E, \mathcal{L}_1\right) \mathcal{B}_{\bar{q}/N}\left(x_2, b, \mu, \frac{\zeta_2}{\nu^2}\right) S(b,\mu,\nu)\,.$$

We further isolate the effects in the partonic scattering cross section and effective Glauber gluon density

$$\mathcal{B}_{q/p,1} = \sum_{i=q,g} \sum_{j=q,\bar{q},g} \sigma_{ij\to q} \otimes f_{i/p} \otimes f_{j/N} \cdot \rho_0^- L^+\,,$$

Structure of the partonic cross section (quark example)

$$\begin{aligned}\sigma^{(0)}_{q/q,T} + \sigma^{(1)}_{q/q,T} = &\left(\mathcal{J}^{(0)}_{q/q,F} + \mathcal{J}^{(1),\rm rap}_{q/q,F}\right) \otimes \Sigma^{(0)}_{FT} \otimes \mathcal{N}^{(0)}_T + \\ &+ \mathcal{J}^{(1),\rm coll}_{q/q,F} \otimes \Sigma^{(0)}_{FT} \otimes \mathcal{N}^{(0)}_T + \mathcal{J}^{(1),\rm coll}_{q/q,A} \otimes \Sigma^{(0)}_{AT} \otimes \mathcal{N}^{(0)}_T \\ &+ \mathcal{J}^{(1),\rm rap}_{q/q,A} \otimes \Sigma^{(0)}_{AT} \otimes \mathcal{N}^{(0)}_T + \mathcal{J}^{(0)}_{q/q,F} \otimes \Sigma^{(1)}_{FT} \otimes \mathcal{N}^{(0)}_T + \mathcal{J}^{(0)}_{q/q,F} \otimes \Sigma^{(0)}_{FT} \otimes \mathcal{N}^{(1)}_T \\ &+ \Delta\sigma^{\rm NLO}_{q/q,T}\,,\end{aligned}$$

- **Tree level terms**
- **Collinear divergences**
- **Rapidity divergences**
- **Soft radiation and anti-collinear**

Fixed order piece

The LPM effect

Before we dive into the calculation, we need to consider coherence in the emission process on a nuclear target

$$\Phi_n = 1 - \frac{\sin\left(\frac{\mathbf{Q}_n^2 L^+}{2x(1-x)p_1^+}\right)}{\frac{\mathbf{Q}_n^2 L^+}{2x(1-x)p_1^+}} \qquad \tau_f = \frac{1}{p^-} = \frac{x(1-x)p^+}{\mathbf{p}^2}$$

L. Landau et al. (1953)

A. Migdal (1956)

The non-trivial scales

"Standard scale ordering"

$$\Lambda^2_{\rm QCD} \ll \mu_E^2 \ll Q^2$$

$$\sqrt{\zeta_1}/\Lambda^2_{\rm QCD} \gg L^+ \gg \sqrt{\zeta_1}/Q^2.$$

- Kinematics suggests that we have dominant contributions from the first scenario
- We consider both and provide formulas that interpolate

Long formation times

$\mu_E \gg \mu_b \qquad \ln(\mu_b^2/\Lambda^2_{\rm QCD})$

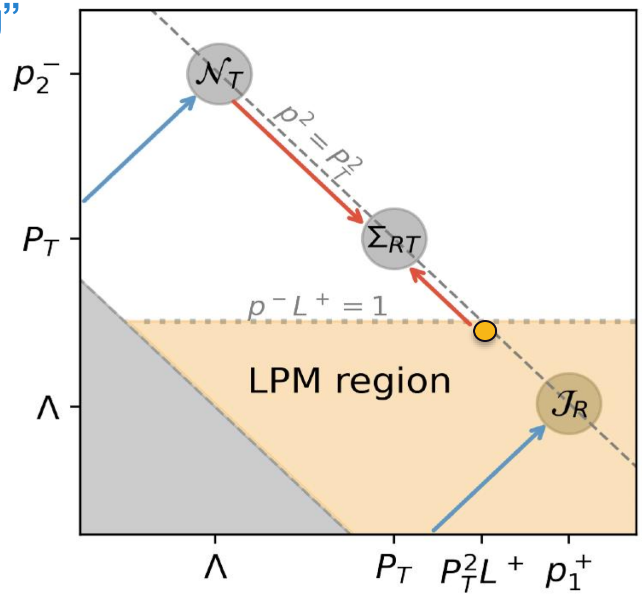

The collinear emission is in the LPM region. Evolution space limited

Short formation times

$\mu_E \ll \mu_b \qquad \ln(\mu_E^2/\Lambda^2_{\rm QCD})$

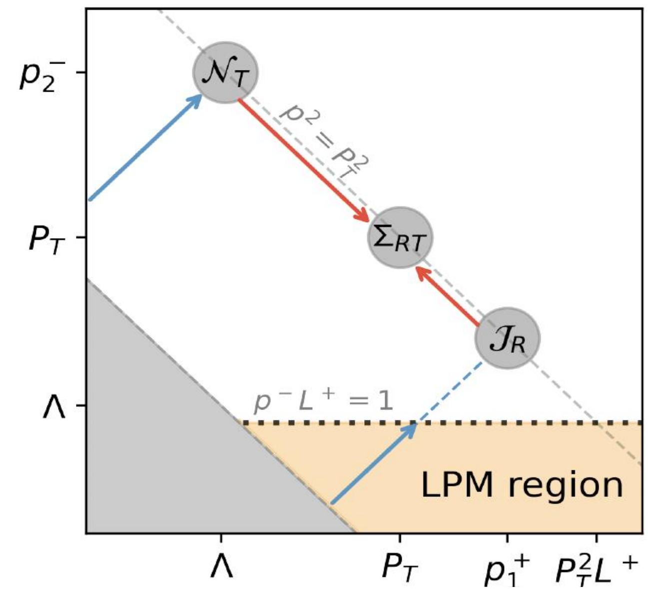

The collinear emission is outside LPM region. Evolution space not limited

Collinear function results

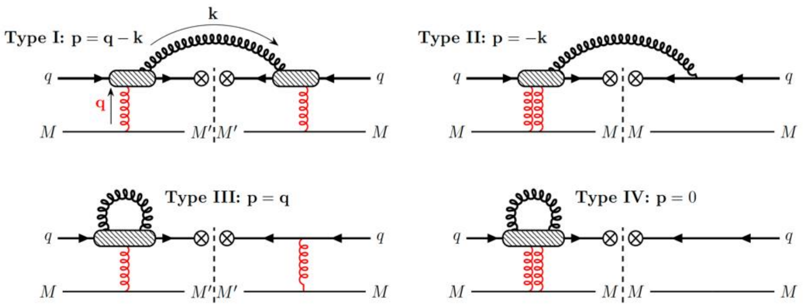

The 4 classes of diagrams contribute differently to the longitudinal and transverse momentum flow in the DY the process

Flavor sum rule explicitly satisfied

$$\int_0^1 dx \int d^2\mathbf{p} \int d^2\mathbf{q}\,\mathcal{J}^{(1)}_{q/q,R}(x,\mathbf{p},\mathbf{q}) = 0$$

$$\mathcal{J}^{(1)}_{q/q,R}(x,\mathbf{p},\mathbf{q}) = \frac{g_s^2 C_F}{2\pi} P_{qq}(x) \int d^2\mathbf{k} \left[\delta^{(2)}(\mathbf{p}-\mathbf{q}+\mathbf{k})\mathcal{I}_{\mathrm{I,R}}(x,\mathbf{p},\mathbf{q}) + \delta^{(2)}(\mathbf{p}+\mathbf{k})\mathcal{I}_{\mathrm{II,R}}(x,\mathbf{p},\mathbf{q})\right]$$
$$+ \frac{g_s^2 C_F}{2\pi}\delta(1-x)\int_0^1 dx' P_{qq}(x') \int d^2\mathbf{k} \left[\delta^{(2)}(\mathbf{p}-\mathbf{q})\mathcal{I}_{\mathrm{III,R}}(x',\mathbf{k},\mathbf{q}) + \delta^{(2)}(\mathbf{p})\mathcal{I}_{\mathrm{IV,R}}(x',\mathbf{k},\mathbf{q})\right].$$

- With kinematic variable definitions, they are given explicitly and with the LPM effect

$$\mathbf{Q}_1 = x\mathbf{k} - (1-x)(\mathbf{p}_0 - \mathbf{k}),$$
$$\mathbf{Q}_2 = x\mathbf{k} - (1-x)(\mathbf{p}_0 - \mathbf{k} + \mathbf{q}),$$
$$\mathbf{Q}_3 = x(\mathbf{k}-\mathbf{q}) - (1-x)(\mathbf{p}_0 - \mathbf{k} + \mathbf{q}),$$
$$\mathbf{Q}_4 = x(\mathbf{k}+\mathbf{q}) - (1-x)(\mathbf{p}_0 - \mathbf{k}),$$

Type K	$\mathcal{I}_F^K(x,\mathbf{k},\mathbf{q})$	$\mathcal{I}_A^K(x,\mathbf{k},\mathbf{q})$
I	$\frac{1}{\mathbf{Q}_1^2} + 2\frac{\mathbf{Q}_2}{\mathbf{Q}_2^2}\cdot\left(\frac{\mathbf{Q}_2}{\mathbf{Q}_2^2} - \frac{\mathbf{Q}_1}{\mathbf{Q}_1^2}\right)\Phi_2$	$\frac{1}{\mathbf{Q}_3^2} - \frac{\mathbf{Q}_1}{\mathbf{Q}_1^2}\cdot\frac{\mathbf{Q}_3}{\mathbf{Q}_3^2} + \frac{\mathbf{Q}_2}{\mathbf{Q}_2^2}\cdot\left(\frac{\mathbf{Q}_1}{\mathbf{Q}_1^2} - \frac{\mathbf{Q}_3}{\mathbf{Q}_3^2}\right)\Phi_2$
II	$-\frac{1}{\mathbf{Q}_1^2}$	$\frac{\mathbf{Q}_1}{\mathbf{Q}_1^2}\cdot\left(\frac{\mathbf{Q}_1}{\mathbf{Q}_1^2} - \frac{\mathbf{Q}_3}{\mathbf{Q}_3^2}\right)(\Phi_1 - 1)$
III	$-2\frac{\mathbf{Q}_2}{\mathbf{Q}_2^2}\cdot\left(\frac{\mathbf{Q}_2}{\mathbf{Q}_2^2} - \frac{\mathbf{Q}_1}{\mathbf{Q}_1^2}\right)\Phi_2$	$-\frac{\mathbf{Q}_1\cdot\mathbf{Q}_2}{\mathbf{Q}_1^2\mathbf{Q}_2^2}\Phi_2 + \frac{\mathbf{Q}_2}{\mathbf{Q}_2^2}\cdot\frac{\mathbf{Q}_4}{\mathbf{Q}_4^2}\Phi_4$
IV	0	$-\frac{1}{\mathbf{Q}_1^2}\Phi_1 + \frac{\mathbf{Q}_1\cdot\mathbf{Q}_5}{\mathbf{Q}_1^2\mathbf{Q}_5^2}\Phi_5$

- The important part is how to identify and treat collinear and rapidity divergences and derive renormalization group equations

The TMD parton energy loss

- We can identify the energy loss of the parton (driven by soft emission)

$$\Delta p_1^+\big|_{\mu_E \ll \mu_b} = \frac{B(w)\rho_G^-(L^+)^2}{8}\frac{4\pi}{\beta_0}\left[\alpha_s(\xi^2) - \alpha_s\left(\gamma(w)\mu_E^2\right)\right]$$

Collinear (or unrestricted phase space case)

$$\Delta p_1^+\big|_{\mu_b \ll \mu_E} \approx \frac{2}{3\pi}\frac{\mu_b^2}{\mu_E^2}\frac{\rho_G^-(L^+)^2}{8}\frac{4\pi}{\beta_0}\left[\alpha_s(\xi^2) - \alpha_s\left(2e^{-1}\mu_b^2\right)\right]$$

TMD (or unrestricted phase space case)

Because

$$B(w \ll 1) \approx \frac{2}{3\pi}\frac{\mu_b^2}{\mu_E^2}, \quad \gamma(w \ll 1) \approx \frac{2}{e}\frac{\mu_b^2}{\mu_E^2}.$$

Energy loss differs between collinear and TMD observables

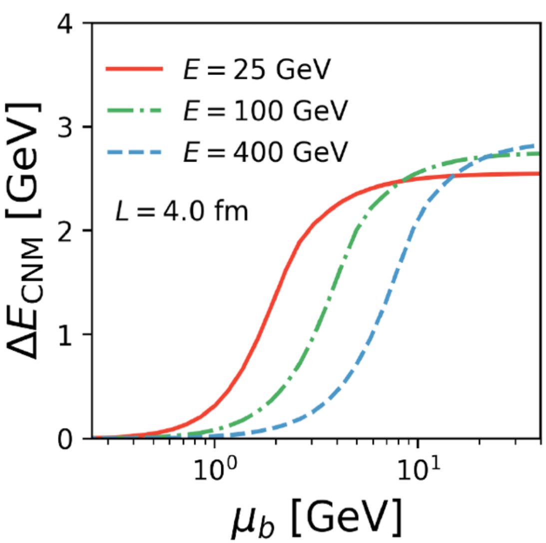

E-loss vs energy

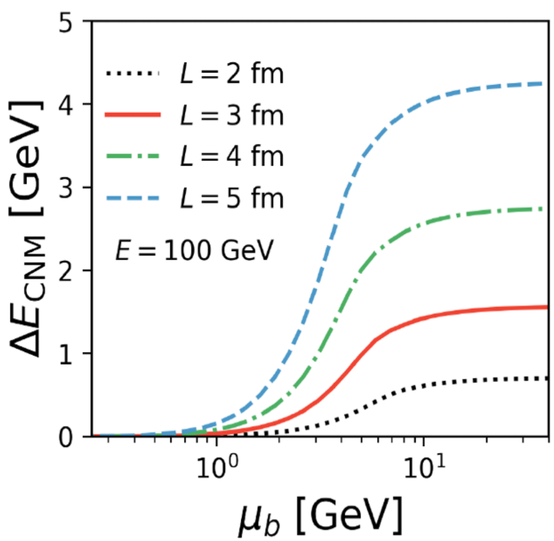

E-loss vs size

Recall the functions

$$B(w) = \frac{4}{\pi}\int_0^w \Phi(x)\frac{dx}{x^2}, \qquad w = \mu_b^2/\mu_E^2,$$

$$\gamma(w) = 2\exp\left\{\frac{1}{B(w)}\frac{4}{\pi}\int_0^w \Phi(x)\ln(x)\frac{dx}{x^2}\right\}$$

Rapidity divergences

Collinear radiation can also lead to rapidity divergences

$$\eta(x) = \left(\frac{(1-x)p_1^+}{\nu}\right)^{-\tau}$$

η regulator

- Regulated by the **η** regulator. Rapidity divergences appear as 1/**τ** poles

$$\mathcal{J}^{(1),\mathrm{rap}}_{q/q,A} \otimes \Sigma^{(0)}_{AT} \otimes \mathcal{N}^{(0)}_{T} \quad = \delta(1-x)\left[-\frac{1}{\tau} + \mathcal{L}_n + \mathcal{O}(\tau)\right] \int \frac{d^{2-2\epsilon}\mathbf{q}}{(2\pi)^{2-2\epsilon}} \hat{\mathcal{C}}\left[\frac{e^{-i\mathbf{q}\cdot\mathbf{b}}}{\mathbf{q}^2}\right] \mathbf{q}^2 \frac{d\sigma^{(0)}_{FT}}{d^2\mathbf{q}} \,,$$

- The LPM effect leads to the appearance of a new Collins-Soper (CS) scale ~ $\mu_b^2 L^+/2$. The LPM effect on RG and RRG connected
- The rapidity logarithm becomes

$$\mathcal{L}_n = \ln \frac{\min\{2L^+\mu_b^2, x_1 P_a^+\}}{\nu}$$

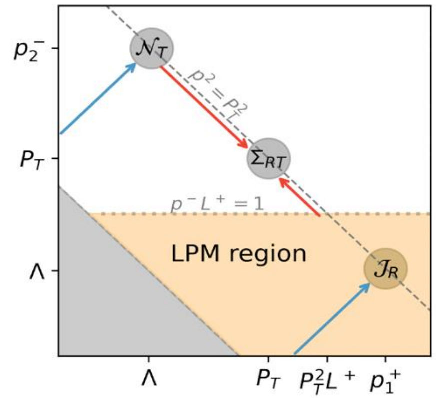

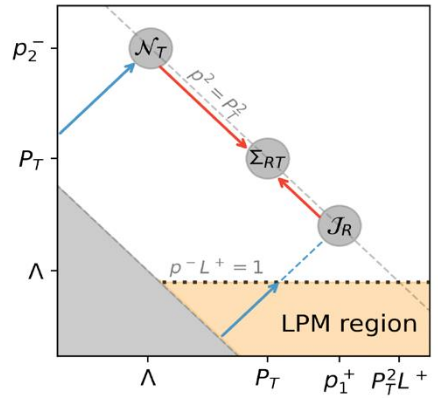

We see the appearance of the BFKL kernel [with action defined on v(q²)]

$$\hat{\mathcal{C}}[v(\mathbf{q}^2)] = \frac{g_s^2 C_A}{\pi} \int \frac{d^{2-2\epsilon}\mathbf{k}}{(2\pi)^{2-2\epsilon}} \left[\frac{1}{(\mathbf{q}-\mathbf{k})^2} v(\mathbf{k}^2) - \frac{\mathbf{q}^2}{2\mathbf{k}^2(\mathbf{q}-\mathbf{k})^2} v(\mathbf{q}^2)\right]$$

To cancel the rapidity pole we need to to consider the soft emission form the Glauber scattering and the target ant-collinear sector

Contributions with rapidity divergences

NLO correction to the Glauber cross section $\Sigma^{(1)}$

We consider soft gluon emission

$$k^\mu \sim (\lambda, \lambda, \lambda) \qquad \left|\frac{k_z}{\nu}\right|^{-\tau/2} = \left|\frac{k^+ - k^-}{2\nu}\right|^{-\tau/2}$$

- There are other diagrams that look like Glauber self energies and wavefunction renormalization. Do not contain rapidity divergences

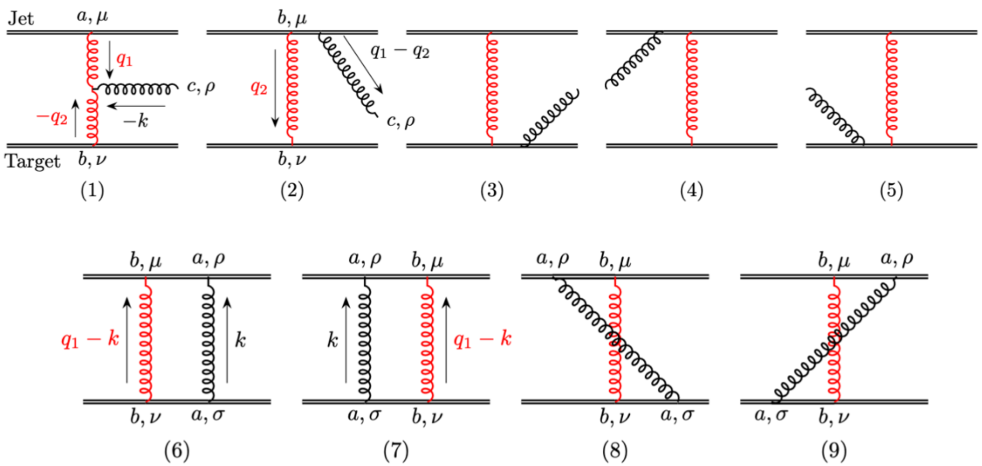

Real and virtual diagrams that contain rapidity divergence

$$\mathcal{J}^{(0)}_{q/q,F} \otimes \Sigma^{(1)}_{FT} \otimes \mathcal{N}^{(0)}_T$$

$$= \int \frac{d^{2-2\epsilon}\mathbf{p}}{(2\pi)^{-2\epsilon}} e^{-i\mathbf{p}\cdot\mathbf{b}} \int \frac{d^{2-2\epsilon}\mathbf{q}}{(2\pi)^{2-2\epsilon}} \int \frac{d^{2-2\epsilon}\mathbf{q}'}{(2\pi)^{2-2\epsilon}} \frac{\mathcal{J}^{(0)}_{q/q,F}}{\mathbf{q}^2} \left(\frac{2}{\tau} + \mathcal{L}_s\right) \hat{\mathcal{C}}\left[\mathbf{q}^2\mathbf{q}'^2\Sigma^{(0)}_{FT}\right] \frac{\mathcal{N}^{(0)}_T}{\mathbf{q}'^2};$$

- Observe the BFKL kernel, pole, and a different soft logarithm $\mathcal{L}_s = \ln\frac{\nu^2}{\mu_b^2}$

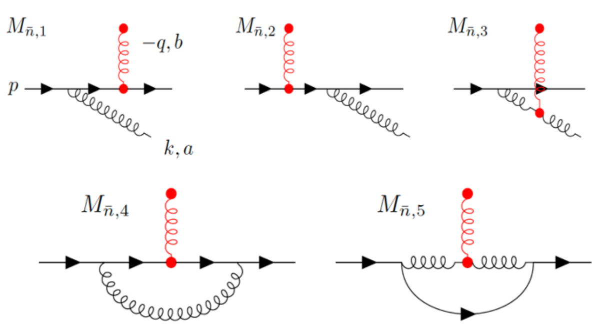

NLO correction from the anti-collinear sector $\mathcal{N}_T^{(1)}$

Note that real emission diagrams contribute. These are not the partons in the large Q process. Double Glauber will not put them off-shell

Cancelation of the rapidity divergences

Putting all sectors together we find that

- The $1/\tau$ poles have cancelled
- The logarithms have combined to become

$$\mathcal{J}^{(0)}_{q/q,F} \otimes \Sigma^{(1)}_{FT} \otimes \mathcal{N}^{(0)}_T + \mathcal{J}^{(1),\mathrm{rap}}_{q/q,A} \otimes \Sigma^{(0)}_{AT} \otimes \mathcal{N}^{(0)}_T$$

$$+ \mathcal{J}^{(0)}_{q/q,F} \otimes \Sigma^{(1)}_{FT} \otimes \mathcal{N}^{(0)}_T + \mathcal{J}^{(0)}_{q/q,F} \otimes \Sigma^{(0)}_{FT} \otimes \mathcal{N}^{(1)}_T$$

$$= \delta(1-x)\frac{g_s^2 C_F g_s^2 C_T}{d_A} \int \frac{d^{2-2\epsilon}\mathbf{q}}{(2\pi)^{2-2\epsilon}} e^{i\mathbf{q}\cdot\mathbf{b}} \frac{1}{\mathbf{q}^2}\left[1 + \mathcal{L}_1 \hat{\mathcal{C}}\right]\frac{1}{\mathbf{q}^2}.$$

$$\mathcal{L}_1 = \ln\left(\min\left\{4x_t m_N L, \frac{x_1 x_t s}{\mu_b^2}\right\}\right) = \ln\left(\min\left\{4m_N L, \frac{x_1 s}{\mu_b^2}\right\}\right) + \ln x_t$$

More thought should be given for phenomenological studies

We can write down the the BFKL-type evolution for the cross section components

$$\frac{g_s^2}{\mathbf{q}^2}\frac{\partial \mathcal{J}_R(x,\mathbf{p},\mathbf{q};\nu)}{\partial \ln \nu} = -\hat{\mathcal{C}}\left[\frac{g_s^2}{\mathbf{q}^2}\mathcal{J}_R(x,\mathbf{p},\mathbf{q};\nu)\right],$$

$$\frac{g_s^2}{\mathbf{q}'^2}\frac{\partial \mathcal{N}_T(\mathbf{q}';\nu')}{\partial \ln \nu'} = -\hat{\mathcal{C}}\left[\frac{g_s^2}{\mathbf{q}'^2}\mathcal{N}_T(\mathbf{q}';\nu')\right],$$

Keep at their scales

Put all BFKL evolution in the Σ

$$\left(\frac{g_s^2}{\mathbf{q}^2}\right)^{-1}\left(\frac{g_s^2}{\mathbf{q}'^2}\right)^{-1}\frac{\partial \Sigma_{RT}(\mathbf{q},\mathbf{q}';\nu,\nu')}{\partial \ln \nu} = \hat{\mathcal{C}}\left[\left(\frac{g_s^2}{\mathbf{q}^2}\right)^{-1}\left(\frac{g_s^2}{\mathbf{q}'^2}\right)^{-1}\Sigma_{RT}(\mathbf{q},\mathbf{q}';\nu,\nu')\right]$$

- A similar equation can be written in v' for the target

$$\text{from } \nu = \min\{2L^+\mu_b^2, x_1 P_a^+\} \ (\nu' = x_t P_b^-) \text{ to } \nu = \mu_b \ (\nu' = \mu_b)$$

BFKL equations solver

Used our own numerical BFKL equation solver in impact parameter space

$$\frac{\partial \tilde{v}(\mathbf{b},\mu)}{\partial y} = \frac{\alpha_s(\mu^2)C_A}{\pi}\Bigg(\tilde{v}(\mathbf{b},\mu)\ln R^2 + \int_{|\mathbf{b}-\mathbf{b}'|>R|\mathbf{b}|}\frac{d^2\mathbf{b}'}{\pi}\frac{\tilde{v}(\mathbf{b}',\mu)}{|\mathbf{b}-\mathbf{b}'|^2} + \int_{|\mathbf{b}-\mathbf{b}'|<R|\mathbf{b}|}\frac{d^2\mathbf{b}'}{\pi}\frac{\tilde{v}(\mathbf{b}',\mu)-\tilde{v}(\mathbf{b},\mu)}{|\mathbf{b}-\mathbf{b}'|^2}\Bigg),$$

One needs to introduce separation parameter R as we have integration over b'
Can be shown that the result does not depend on R

W. Ke et al. (2024)

- Initial condition that interpolates beet the vacuum case and the medium case

$$\tilde{v}_T(\mathbf{b}; y=0) = 2\pi\frac{\alpha_s\left(\mu_b^2+\xi^2\right)C_T}{\pi}K_0\left(b\sqrt{\mu_b^2+\xi^2}\right)$$

Matched to the DLA initial condition (y=0) at ξb=0.35

Analytic solution comparison in the DLA approximation

$$\tilde{v}_T^{\mathrm{DLA}}(\mathbf{b};y) = C_0 e^{(\alpha_P-1)y}\int\frac{d^2\mathbf{q}}{(2\pi^2)}\frac{e^{-i\mathbf{b}\cdot\mathbf{q}}}{2|\mathbf{q}|\xi}\frac{e^{-\frac{[\ln|\mathbf{q}|-\ln\xi]^2}{2\sigma^2 y}}}{\sqrt{2\pi\sigma^2 y}}$$

Parameters $\alpha_P - 1 = \frac{\alpha_{s,\mathrm{fix}}C_A}{\pi}4\ln 2,\ \sigma = 7\zeta(3)\frac{\alpha_{s,\mathrm{fix}}C_A}{\pi}y.$

- Matches well after a few units in rapidity. Looses memory of initial conditions

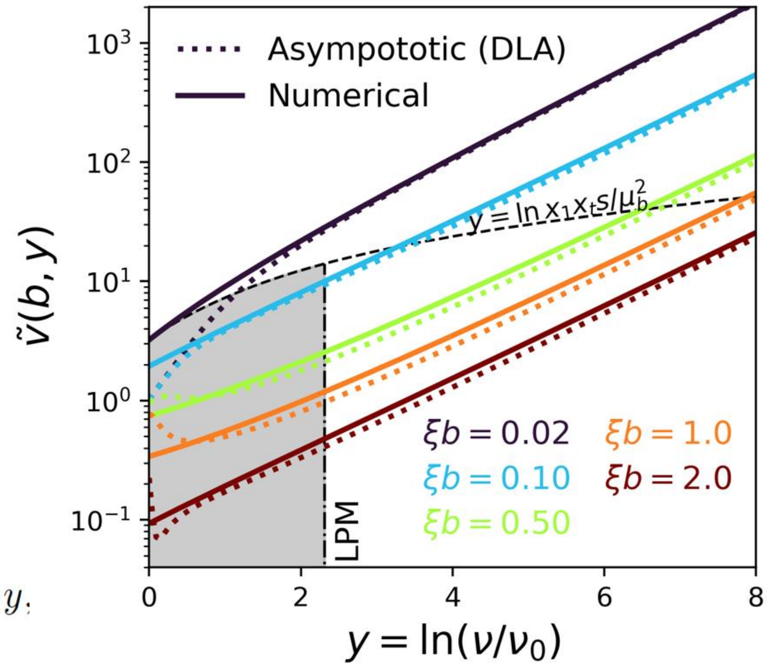

BFKL solution compared to the asymptotic case

The final result

Modified p beam function

$$\mathcal{B}^{\rm CNM}_{q/a}\left(x_1, b, \mu, \frac{\zeta_1}{\nu^2}; \mu_E, \mathcal{L}_1\right) = \sum_i \int_{x_1}^1 \frac{dx}{x} f_{i/a}\left(\frac{x_1}{x}, \mu_b^*, \mu_E\right) C_{q/i}\left(x, b, \mu_b^*, \frac{\zeta_1}{\nu^2}\right) e^{-S^f_{\rm NP}(b,\zeta_1)}$$

$$\times \exp\left\{\rho_0^- L^+ \sum_j \int dx_t f_{j/N}(x_t) \left[\tilde{\Sigma}_{ij}(b, \mathcal{L}_1) - \tilde{\Sigma}_{ij}(0, \mathcal{L}_1)\right]\right\}$$

$$\times \left(1 + \rho_0^- L^+ \sum_j \int dx_t f_{j/N}(x_t) \Delta\sigma^{\rm NLO}_{ij\to q}\right) .$$

- Collinear evolution (RG) modifies the PDF in the proton (including LPM).
- Multiple Glauber gluons exponentiate (including unitarity corrections)
- Radiation enhances broadening, renormalizes (RRG) the forward scattering cross section.
- There are finite contributions

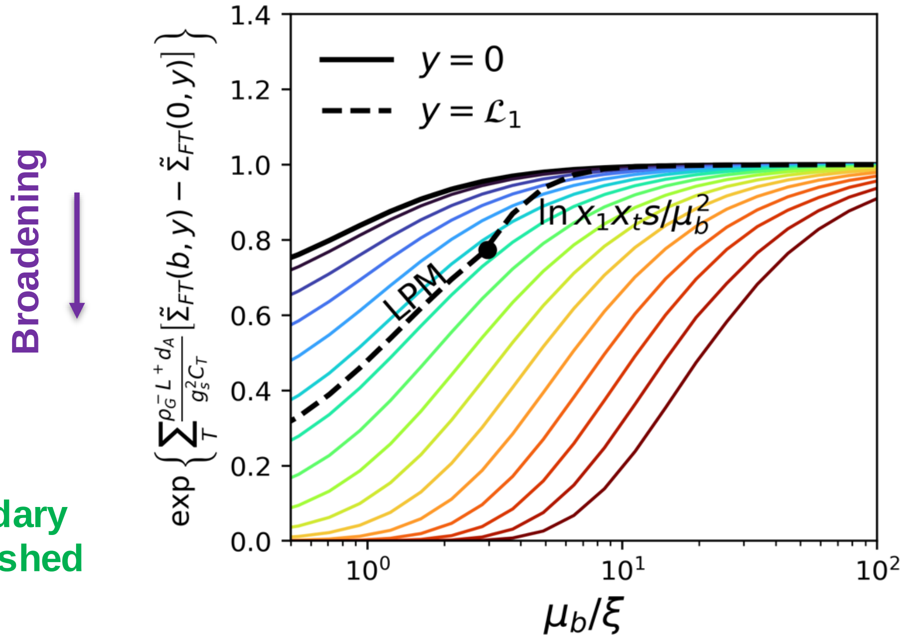

Rapidity evolution of the forward scattering in impact parameter space. Solid line is the boundary condition from tree level Glauber exchange, dashed – the physical boundary.

Effective modification of the TMD distribution in pA

- Rich stricture appears from CNM effects in 3D proton beam function. Note that scales are set differently then in collinear factorization and reflected on results
- Will affect significantly global extraction

M. Alrashed et al. (2021)

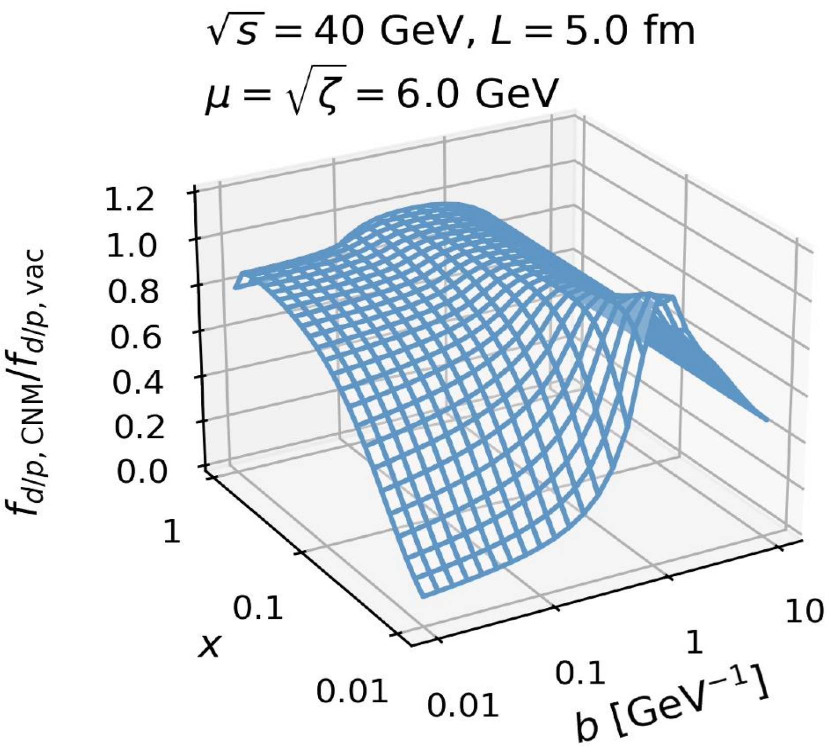

Impact parameter space

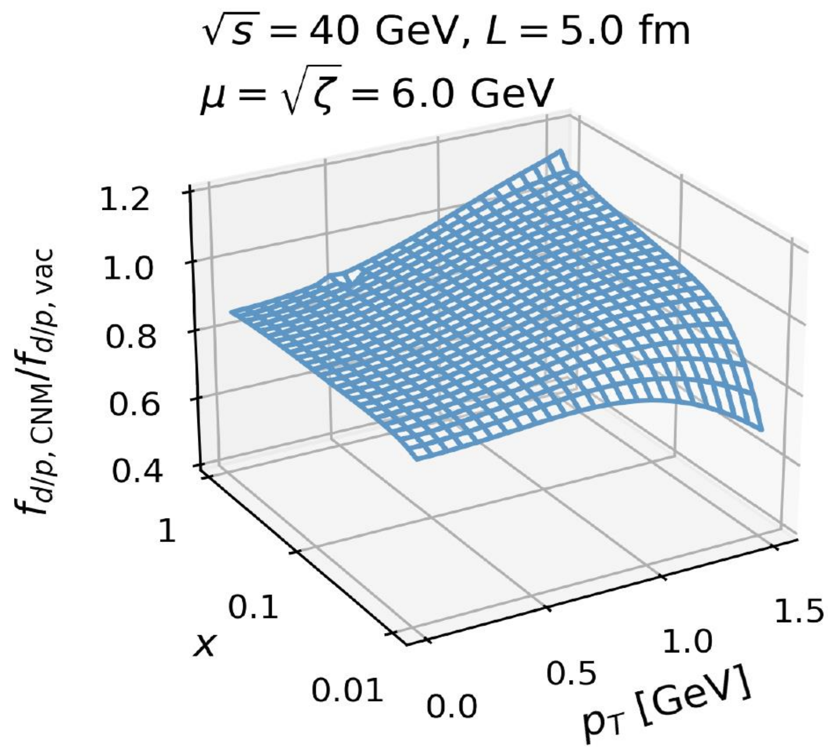

Momentum space

One has to be careful pushing to x ~ 0.01 and below as one enters a regime of coherent scattering with the target that we did not explicitly consider

Phenomenological results – collider energies and PHENIX data

Look at the nuclear modification factor for DY production at small transverse momenta

$$R_{pA} = \frac{1}{A}\frac{d\sigma_{pA}/dQ^2dydp_T}{d\sigma_{pp}/dQ^2dydp_T}$$

- Isospin gets a little separation in R_{pA} for forward and backward rapidities
- Collisional broadening and radiation lead to further separation
- Including nPDF at scale p_T has an effect on the R_{pA} shape

- Not clear if shape or norm is more important
- When we go to backward rapidity we enter a region of scales where the calculation breaks earlier
- There is no Y term to match at high p_T and scale setting

W. Ke et al. (2024)

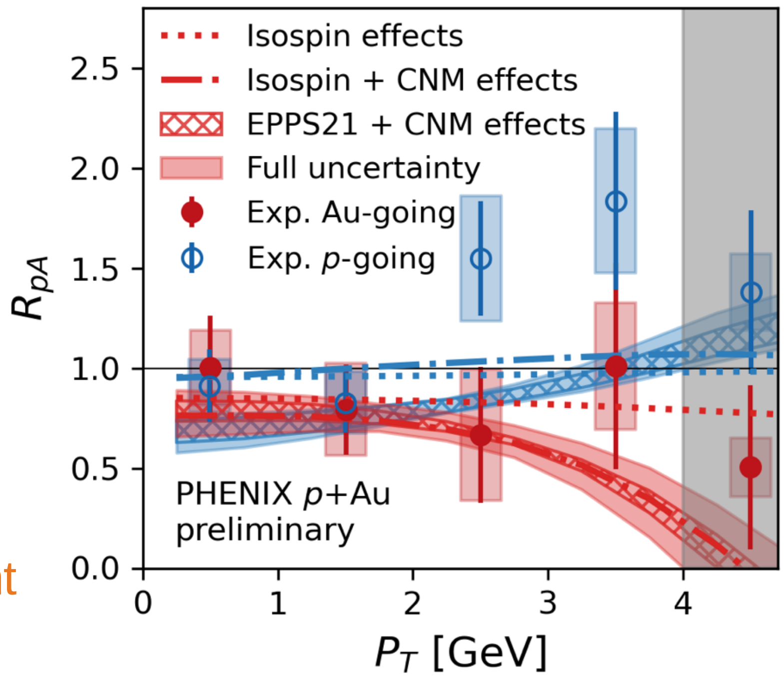

Comparison to PHENIX data (which has remained preliminary for quite some time)

Y. Leung et al. (2019)

The error bars have remained quite large in this measurement. Look at more precise fixed target measurements form Fermilab

Phenomenological results – fixed target energies and E866 data

Fixed target experiment data E866 provides ratios of nuclear targets

- The calculation captures the mass dependence
- The nuclear effects derived here are important for a better description of the transition from suppression to enhancement
- Opens the door to phenomenology

M. Vasiliev et al. (1999)

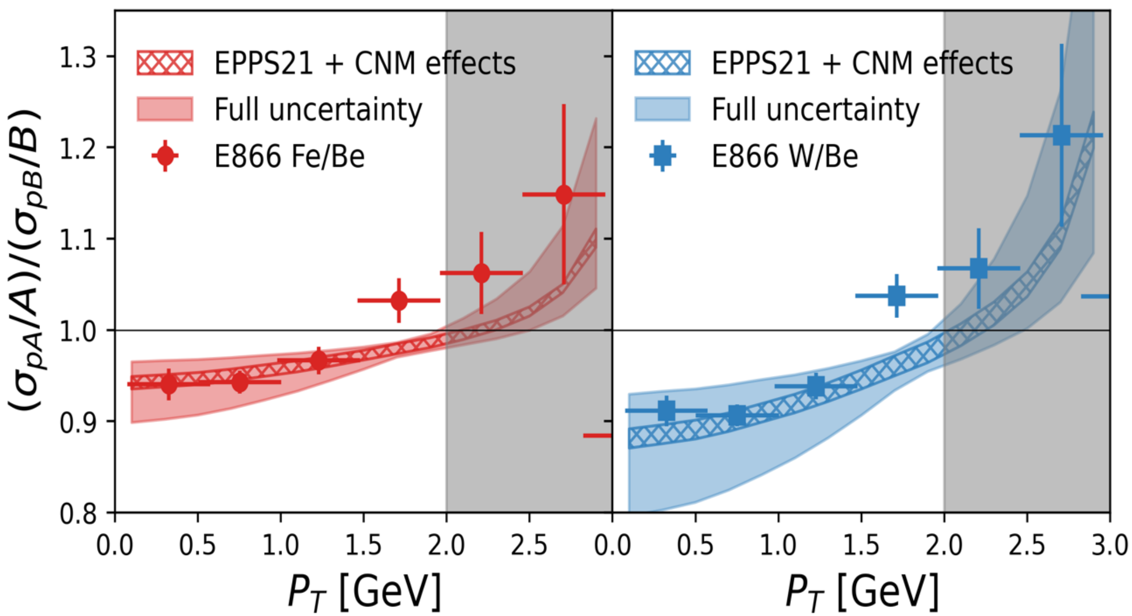

Nuclear size dependence and uncertainties

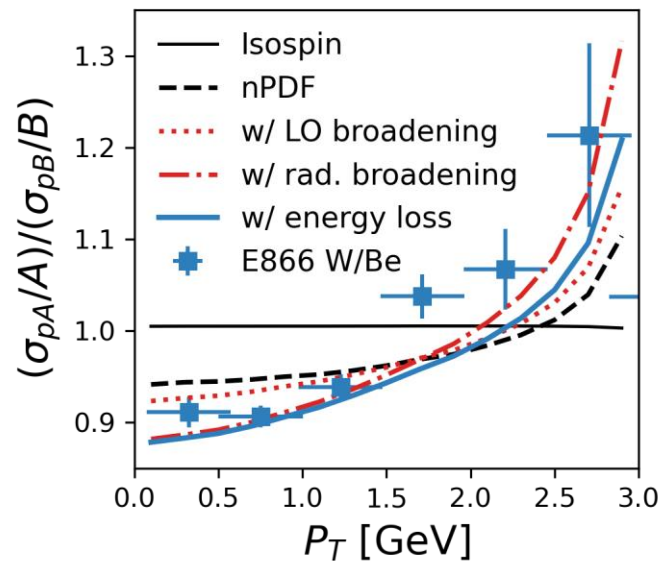

Contribution of various effects

Conclusions

- Many of the cold nuclear matter effects can be understood from the formation anad evolution of in-medium parton showers. Resummation of large nuclear matter induced logarithms is essential to interpret the results from reactions with nuclei
- Other approaches exist, however analytic insights have thus far been absent. We developed an RG evolution approach that overcomes this limitation. It is fast, efficient, improvable, and represents an important rigorous theoretical development in the literature.
- We first applied it to collinear factorization, exemplified by SIDIS, to derive a novel set of in-medium evolution equations. Understood analytically parton shower energy loss. Demonstrated applications to phenomenology – HERMES, EMC and EIC.
- We extended the in-medium RG formalism to TMD factorization on the example of DY, unifying broadening and radiative corrections
- In addition to RG evolution, we derived rapidity renormalization group equations (RRG) that take into account the LPM effect. It is essential in limiting the fast BFKL growth of target density
- With partial exponentiation to higher orders in opacity applied to phenomenology. Partial success, but also identifying the limitations and direction for future, from scale setting, to better understanding the rapidity log and matching to the collinear formalism
- The tensions also helped us identify the limitations and direction for future, from scale setting, to better understanding the rapidity log and matching to the collinear formalism